Inorg. Chem. **2002**, *41*, 4051−4057

Antimony Ethylene Glycolate and Catecholate Compounds: Structural Characterization of Polyesterification Catalysts

Shannon M. Biros, Brian M. Bridgewater, Adriel Villeges-Estrada, Joseph M. Tanski, and Gerard Parkin*

Department of Chemistry, Columbia University, New York, New York 10027

Received March 14, 2002

Antimony compounds are widely used as catalysts for the synthesis of the commercially important polymer poly(ethyleneterephthalate) by polycondensation of bis(hydroxyethyl)terephthalate. The precise nature of the antimony catalysts is, however, unknown. The present study has been conducted with a view to determining the nature of the catalytic species by structurally characterizing antimony ethylene glycolate compounds and related catecholate derivatives, namely $[Sb_2(OCH_2CH_2O)_3]_n$, $[Sb(OCH_2CH_2O)(OAc)]_n$, $[pySb(1,2\text{-}O_2C_6H_4)]_2O$, and $[pyH][Sb(1,2\text{-}O_2C_6H_4)_2]$.

Introduction

Poly(ethylene terephthalate), PET, is the most common thermoplastic polyester and is manufactured with a variety of brand names, including Dacron, Mylar, and Terylene.[1,2] PET has numerous applications, with more than 85% being processed into fibers, while a significant and growing application of PET is the manufacture of gastight bottles for carbonated beverages. PET is obtained commercially by two methods, both of which involve polycondensation of bis(hydroxyethyl)terephthalate (BHET) but differ in terms of the feedstock (Scheme 1).[1] One method employs dimethyl terephthalate and involves generation of bis(hydroxyethyl)terephthalate by transesterification with ethylene glycol at temperatures of 150−200 °C. This process is catalyzed by a variety of metal complexes (typically acetates of Ca, Mg, Zn, Cd, Pb, or Co), and the methanol released is distilled out of the reaction vessel to shift the equilibrium. A more recent method for generating BHET involves direct esterification of terephthalic acid with ethylene glycol. Regardless of the method and catalysts used to synthesize BHET, antimony-based catalysts are generally considered to be the most efficient for achieving the polycondensation reaction.[3,4]

The most common antimony compound used in these polycondensation reactions is antimony trioxide (Sb_2O_3).[1,4] The detailed mode of action is not known, although it has been suggested that the general role of a polycondensation catalyst is to coordinate the ester carbonyl group of BHET and thereby promote nucleophilic attack by the hydroxyl group of another molecule.[5] However, despite the efficiency of Sb_2O_3, drawbacks to the use of this compound include the formation of side-products (such as acetaldehyde) and catalyst decomposition depositing elemental antimony, which imparts an undesirable gray color to the polymer.[4] As a result, more efficient polyesterification catalysts have been sought. Three such antimony compounds that exhibit polycondensation catalytic activity are antimony triacetate, $Sb(OAc)_3$,[3,4] antimony ethylene glycolate, $[Sb_2(OCH_2CH_2O)_3]_n$,[3,4,6] and the hybrid complex $[Sb(OCH_2CH_2O)(OAc)]_n$.[7] In this report, we describe structural studies on a series of antimony ethylene glycolate and acetate complexes as part of an effort to provide insight into the nature of the species that exist in this catalytic system.

Results and Discussion

1. Molecular Structures of the Ethylene Glycolate Complexes $[Sb_2(OCH_2CH_2O)_3]_n$ and $[Sb(OCH_2CH_2O)(OAc)]_n$. $[Sb_2(OCH_2CH_2O)_3]_n$, which is typically obtained by the reaction of Sb_2O_3 with ethylene glycol,[6] is believed to be the active catalyst component in the condensation polymerization of BHET to PET.[3] However, the molecular structure of $[Sb_2(OCH_2CH_2O)_3]_n$ is unknown, although it has

* To whom correspondence should be addressed. E-mail: parkin@chem.columbia.edu.

(1) *Industrial Polymers Handbook*; Wilks, E. S., Ed.; Wiley-VCH: New York, 2001; Vol. 1, pp 313−322.
(2) Parshall, G. W.; Ittel, S. D. *Homogeneous Catalysis*, 2nd ed.; Wiley: New York, 1992.
(3) Maerov, S. B. *J. Polym. Sci., Polym. Chem. Ed.***1979**, *17*, 4033−4040.
(4) Aharoni, S. M. *Polym. Eng. Sci.* **1998**, *38*, 1039−1047.
(5) Chung, J. S. *J. Macromol. Sci., Chem.* **1990**, *A27*, 479−490.
(6) Mehrota, R. C.; Bhatnagar, D. D. *J. Indian. Chem. Soc.* **1965**, *42*, 327−332.
(7) Loeffler, E. O. U.S. Patent 3,935,170, 1976.

10.1021/ic020204b CCC: $22.00
Published on Web 06/29/2002

Scheme 1

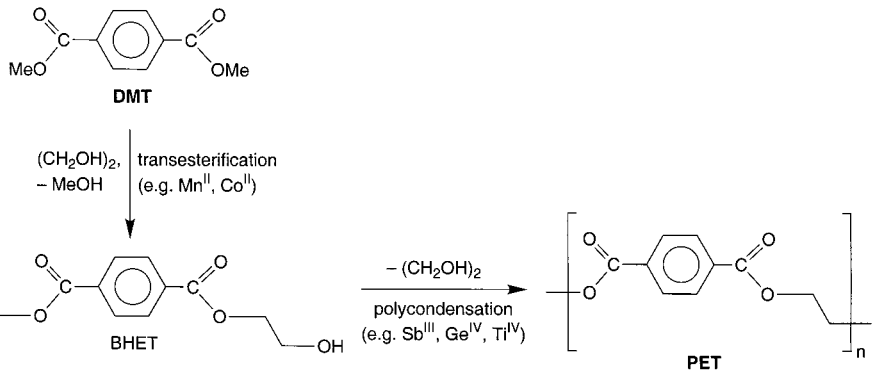

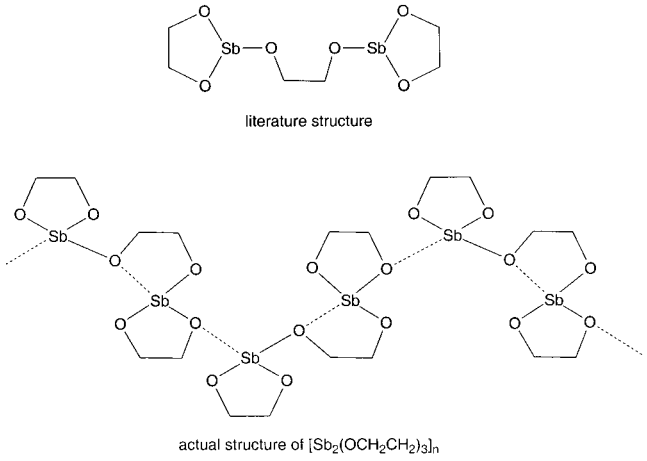

Figure 1. Comparison of the literature representation of the structure of $[Sb_2(OCH_2CH_2O)_3]_n$ and the actual structure.

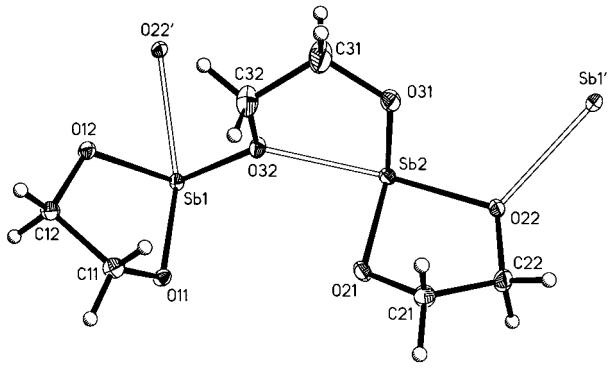

Figure 2. Asymmetric unit of $[Sb_2(OCH_2CH_2O)_3]_n$.

been represented as the discrete dinuclear species illustrated in Figure 1.[3] To determine the precise nature of the structure of $[Sb_2(OCH_2CH_2O)_3]_n$, crystals suitable for X-ray diffraction were obtained by crystallization from hot ethylene glycol. The molecular structure of $[Sb_2(OCH_2CH_2O)_3]_n$ as determined by X-ray diffraction is illustrated in Figure 2. Interestingly, the structure of $[Sb_2(OCH_2CH_2O)_3]_n$ does not

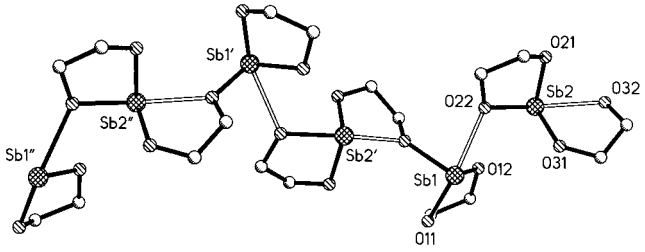

Figure 3. Extended structure of $[Sb_2(OCH_2CH_2O)_3]_n$, emphasizing the one-dimensional chain.

Table 1. Selected Bond Lengths (Å) and Angles (deg) for $[Sb_2(OCH_2CH_2O)_3]_n$

Sb1−O11	2.046(2)	Sb2−O31	1.981(3)
Sb1−O12	2.001(2)	Sb2−O32	2.373(2)
Sb2−O21	2.004(2)	Sb1−O32	2.051(2)
Sb2−O22	2.057(2)	Sb1−O22	2.474(2)
O11−Sb1−O12	80.2(1)	O12−Sb1−O32	95.7(1)
O11−Sb1−O32	88.6(1)	O12−Sb1−O22	68.8(1)
O11−Sb1−O22	144.9(1)	O22−Sb1−O32	78.8(1)
O21−Sb2−O31	96.1(1)	O31−Sb2−O22	86.0(1)
O21−Sb2−O22	79.7(1)	O31−Sb2−O32	75.6(1)
O21−Sb2−O32	82.5(1)	O22−Sb2−O32	152.8(1)

correspond to the dinuclear species represented in Figure 1 but, rather, is polymeric, consisting of one-dimensional chains (Figures 1−3). Unlike the representation in Figure 1, the repeat unit in each chain has two different antimony environments (Figures 1−3), the principal difference of which is the binding mode of the glycolate ligands. Thus, one antimony (Sb1) is coordinated in a bidentate fashion to a single nonbridging glycolate ligand and in a unidentate manner to two bridging glycolate ligands, whereas the other antimony (Sb2) is coordinated in a bidentate fashion to two bridging glycolate ligands (Figures 1 and 2). Despite the difference in glycolate coordination modes, the environment about both antimony centers is similar in terms of the Sb−O bond lengths (Table 1). Specifically, both antimony centers possess three short and one long Sb−O bonds, corresponding to covalent and dative−covalent interactions, respectively

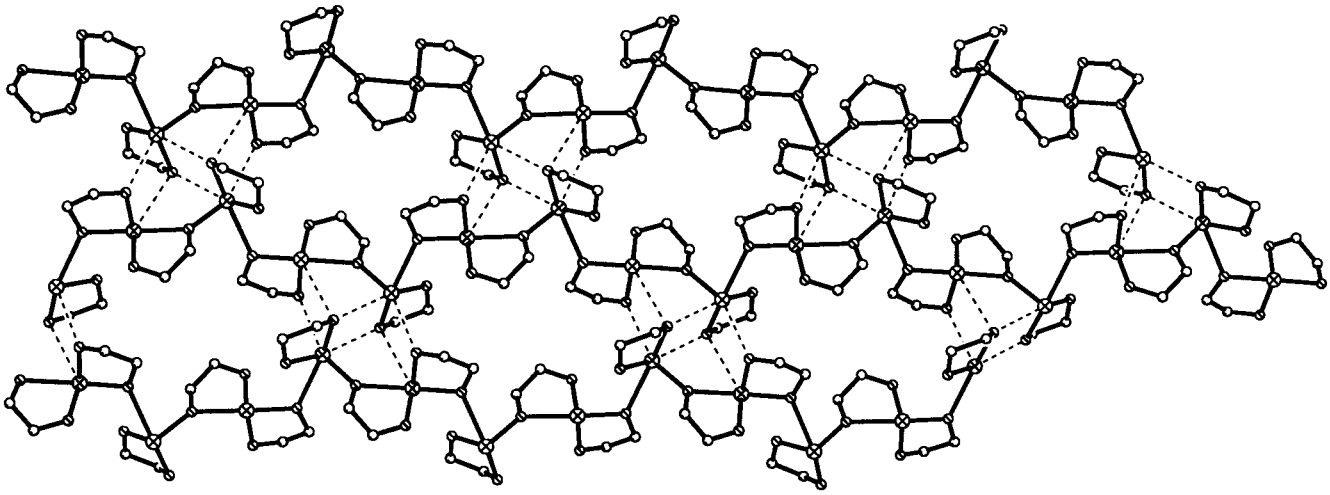

Figure 4. Interaction between the chains of $[Sb_2(OCH_2CH_2O)_3]_n$ forming a two-dimensional sheet.

(Figures 1 and 3);[8] the short Sb−O bond lengths average 2.02 Å, while the long bonds average 2.42 Å (Table 1).

The primary coordination about each antimony in the one-dimensional chain is supplemented by secondary Sb···O interactions between chains that result in the formation of a two-dimensional sheet (Figure 4). Thus, Sb1 contacts O11 and O21 of an adjacent chain at a distance of 2.62 and 2.75 Å, while Sb2 contacts O11 of an adjacent chain at a distance of 2.91 Å. Thus, the Sb−O bond lengths in $[Sb_2(OCH_2CH_2O)_3]_n$ fall into three classes: 2.0 Å (normal covalent), 2.4 Å (dative covalent, intrachain), and 2.6−2.9 Å (interchain). Further comparison, however, is not possible because of the absence of structurally characterized antimony(III) ethylene glycolate complexes in the Cambridge Structural Database.[9−11]

$[Sb(OCH_2CH_2O)(OAc)]_n$, which may be synthesized by the reaction of $Sb(OAc)_3$ with ethylene glycol,[7,12] is also an active catalyst for polycondensation of BHET. The molecular structure of $[Sb(OCH_2CH_2O)(OAc)]_n$, however, was unknown. Nevertheless, several possibilities for the structure $[Sb(OCH_2CH_2O)(OAc)]_n$ were proposed, some of which have antimony centers that are not coordinated to acetate (Figure 5).[7] The previous inability to determine the structure of $[Sb(OCH_2CH_2O)(OAc)]_n$ is undoubtedly a manifestation of its insolubility. To solve this problem, crystals of $[Sb(OCH_2CH_2O)(OAc)]_n$ suitable for X-ray diffraction were obtained by slow diffusion between layers of $Sb(OAc)_3$ in THF and ethylene glycol in THF, separated by an additional layer of

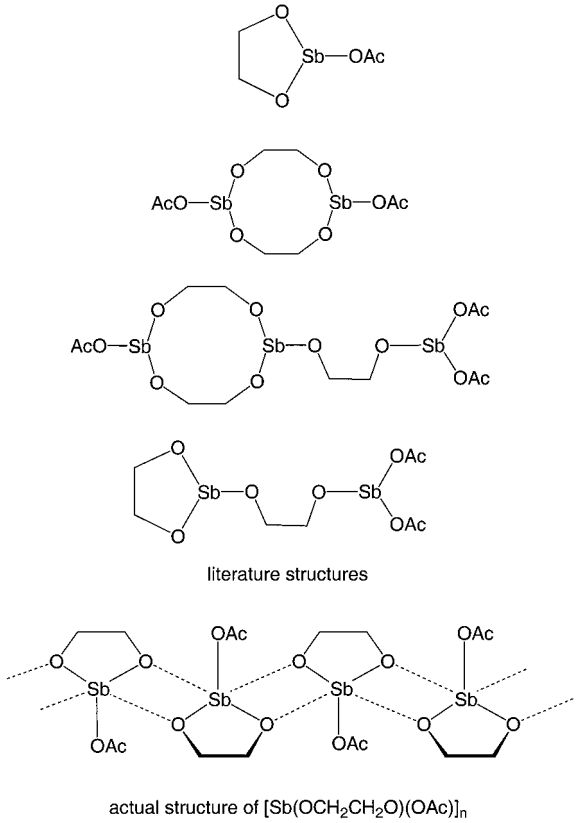

Figure 5. Comparison of the literature representations of the structure of $[Sb(OCH_2CH_2O)(OAc)]_n$ with the actual structure.

THF. The molecular structure of $[Sb(OCH_2CH_2O)(OAc)]_n$, as determined by X-ray diffraction, is illustrated in Figures 5−7. Although the molecular structure of $[Sb(OCH_2CH_2O)(OAc)]_n$ does not correspond directly to any of the previous proposals, each of which involve three-coordinate antimony centers, it is clearly related to the top proposal of Figure 5, that is, $Sb(\eta^2\text{-}OCH_2CH_2O)(OAc)$. Specifically, the structure of $[Sb(OCH_2CH_2O)(OAc)]_n$ consists of a one-dimensional chain in which the oxygen atoms of the glycolate ligand of each $[Sb(OCH_2CH_2O)(OAc)]$ fragment bridge to the antimony centers of two adjacent fragments. The three Sb−O bond lengths within the $[Sb(OCH_2CH_2O)(OAc)]$ fragment

(8) Haaland, A. *Angew. Chem., Int. Ed. Engl.* **1989**, *28*, 992−1000.
(9) CSD Version 5.19, *3D Search and Research Using the Cambridge Structural Database*: Allen, F. H.; Kennard, O. *Chemical Design Automation News* **1993**, *8* (1), 1, 31−37.
(10) For some structurally characterized Sb^V−(OCR_2CR_2O) derivatives, see: (a) Wieber, M.; Baumann, N.; Wunderlich, H.; Rippstein, H. *J. Organomet. Chem.* **1977**, *133*, 183−186. (b) Holmes, R. R.; Day, R. O.; Chandrasekhar, V.; Holmes, J. M. *Inorg. Chem.* **1987**, *26*, 163−168. (c) Fukin, G. K.; Zakharov, L. N.; Domrachev, G. A.; Fedorov, A. Y.; Zaburdyaeva, S. N.; Dodonov, V. A. *Russ. Chem. Bull.* **1999**, *48*, 1722−1732.
(11) An example of a metal−glycolate polymer that has been crystallographically characterized is $[Ti(OCH_2CH_2O)_2]_n$. See: Wang, D.; Yu, R.; Kumada, N.; Kinomura, N. *Chem. Mater.* **1999**, *11*, 2008−2012.
(12) Reaction of $Sb(OAc)_3$ with excess ethylene glycol yields $[Sb_2(OCH_2CH_2O)_3]_n$. See: Loeffler, O. E. U.S. Patent 3,833,630, September 1974.

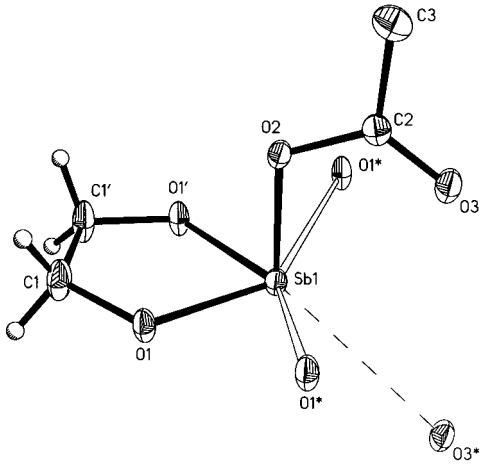

Figure 6. Antimony coordination environment in $[Sb(OCH_2CH_2O)(OAc)]_n$.

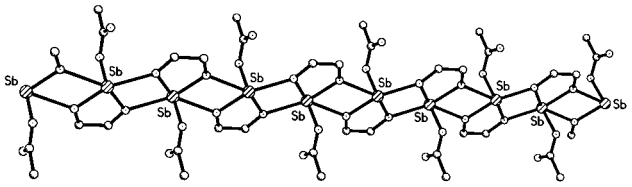

Figure 7. Extended structure of $[Sb(OCH_2CH_2O)(OAc)]_n$, emphasizing the one-dimensional chain.

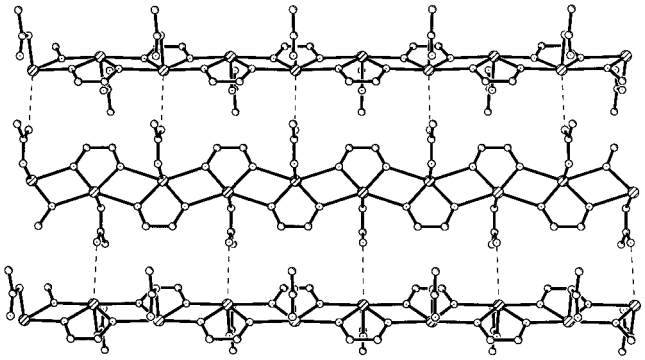

Figure 8. Weak interactions between chains of $[Sb(OCH_2CH_2O)(OAc)]_n$.

Table 2. Selected Bond Lengths (Å) and Angles (deg) for $[Sb(OCH_2CH_2O)(OAc)]_n$

Sb−O1	2.031(3)	Sb−O2	2.035(4)
Sb−O1*	2.470(3)		
O1−Sb−O1′	78.6(2)	O1−Sb−O2	89.3(1)
O1−Sb−O1*	66.8(1)	Sb−O1−Sb	113.2(1)
O1*-Sb−O1*′	144.0(1)	O1*-Sb−O2	81.1(1)

are short, averaging 2.03 Å, while the bridging interaction is long (2.47 Å), as summarized in Table 2. The bridging interactions result in the $[Sb(OCH_2CH_2O)]$ fragment forming a planar array from which the acetate ligands are oriented perpendicularly, in an alternating up/down manner (Figure 7). The uncoordinated oxygen atom of each acetate ligand interacts with antimony atoms of adjacent chains, as illustrated in Figure 8. However, these secondary Sb···O interactions (3.46 Å) are sufficiently close to the sum of the van der Waals radii of Sb and O (3.6 Å)[13] that it is not appropriate to describe $[Sb(OCH_2CH_2O)(OAc)]_n$ as a two-dimensional polymer, and that its classification as a one-dimensional chain is more accurate. Thus, the dimensionality decreases as the ethylene glycolate composition decreases.

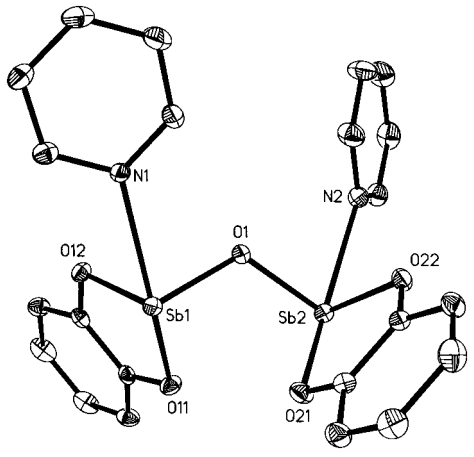

Figure 9. Molecular structure of $[pySb(1,2\text{-}O_2C_6H_4)]_2O$.

Scheme 2

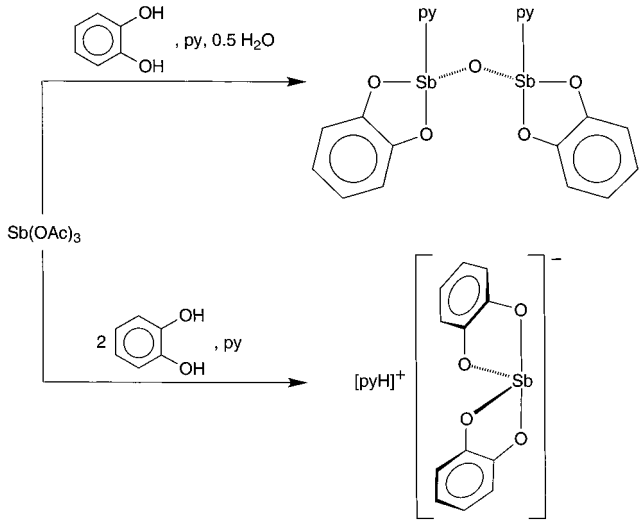

Table 3. Selected Bond Lengths (Å) and Angles (deg) for $[pySb(1,2\text{-}O_2C_6H_4)]_2O$

Sb1−O1	1.982(3)	Sb2−O1	1.962(3)
Sb1−O11	2.084(3)	Sb2−O21	2.090(3)
Sb1−O12	2.038(3)	Sb2−O22	2.045(3)
Sb1−N1	2.486(3)	Sb2−N2	2.453(4)
O11−Sb1−O12	80.5(1)	O21−Sb2−O22	80.1(1)
O1−Sb1−O11	88.1(1)	O1−Sb2−O21	88.1(1)
O1−Sb1−O12	97.8(1)	O1−Sb2−O22	96.6(1)
O1−Sb1−N1	80.4(1)	O1−Sb2−N2	80.5(1)
N1−Sb1−O11	152.6(1)	N2−Sb2−O21	153.8(1)
N1−Sb1−O12	76.6(1)	N2−Sb2−O22	77.9(1)
Sb1−O1−Sb2	118.2(1)		

2. Molecular Structures of the Catecholate Complexes $[pySb(1,2\text{-}O_2C_6H_4)]_2O$ and $[pyH][Sb(1,2\text{-}O_2C_6H_4)_2]$. In addition to studying the structures of antimony ethylene glycolate complexes, we have also examined related catecholate derivatives. Not only do antimony catecholate complexes have potential applications as polycondensation catalysts but they are also of interest with respect to a search for layered antimony(III) complexes.[14] For example, the catecholate compound $[Sb(1,2\text{-}O_2C_6H_4)]_2O$ has been proposed to be a layered material capable of intercalating

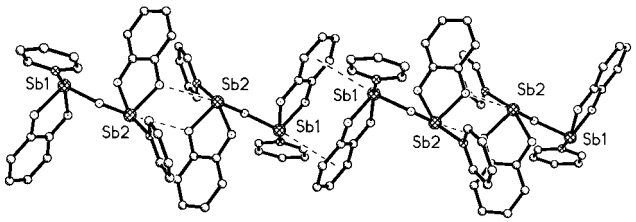

Figure 10. Extended structure of $[pySb(1,2\text{-}O_2C_6H_4)]_2O$.

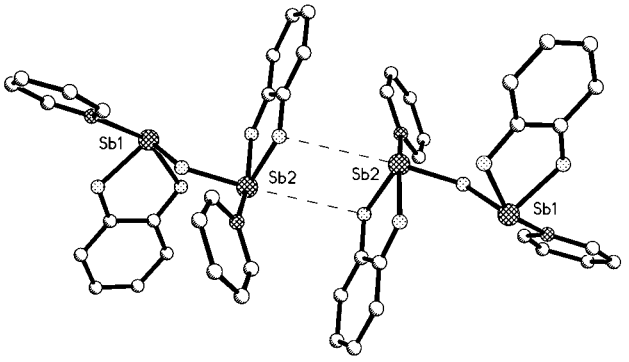

Figure 11. Extended structure of $[pySb(1,2\text{-}O_2C_6H_4)]_2O$, emphasizing the Sb···O interaction.

pyridine.[14] Of interest to this intercalation study, we have observed that the fragment $[Sb(1,2\text{-}O_2C_6H_4)]_2O$ is capable of chemically binding pyridine. Specifically, the pyridine adduct $[pySb(1,2\text{-}O_2C_6H_4)]_2O$ may be obtained by reaction of $Sb(OAc)_3$ with catechol and water in pyridine (Scheme 2). Of potential relevance to the intercalation study, the pyridine may be removed from $[pySb(1,2\text{-}O_2C_6H_4)]_2O$ by heating at 90 °C under vacuum.

The molecular structure of $[pySb(1,2\text{-}O_2C_6H_4)]_2O$ has been determined by X-ray diffraction, demonstrating that each antimony has a distorted trigonal bipyramid geometry, with the oxo ligand occupying an equatorial site, and the pyridine, an axial site (Figure 9).[15] The oxo bridge is distinctly bent [Sb−O−Sb = 118.2(1)°], and the Sb−O bond lengths [1.962(3) and 1.982(3) Å] are marginally shorter than those for the catecholate ligand (2.04−2.09 Å), as summarized in Table 3.

An interesting aspect of the extended structure of $[pySb(1,2\text{-}O_2C_6H_4)]_2O$, as illustrated in Figure 10, is that the two antimony centers supplement the primary bonding by different means. Thus, while one of the antimony centers (Sb2) supplements the bonding by interacting with an oxygen atom (3.43 Å) of an adjacent molecule, resulting in an $[Sb_2O_2]$ rectangular motif (Figure 11), the other antimony interacts with the benzene ring of a catecholate ligand (Figure 12).

(13) The van der Waals radii of Sb and O are 2.2 and 1.4 Å, respectively. See Pauling, L. *The Nature of The Chemical Bond*, 3rd ed.; Cornell University Press: Ithaca, NY, 1960; p 260.

(14) Alonzo, G.; Bertazzi, N.; Galli, P.; Marci, G.; Massacci, M. A.; Palmisano, L.; Patrono, P.; Saiano, F. *Mater. Res. Bull.* **1998**, *33*, 1233−1240.

(15) It should be noted that a second crystalline form of $[pySb(1,2\text{-}O_2C_6H_4)]_2O$ was identified by X-ray diffraction, in which the principal difference is that the pyrdine ligands adopt "trans" positions. Cell parameters: triclinic, $a = 7.60(1)$ Å, $b = 11.46(2)$ Å, $c = 13.56(3)$ Å, $\alpha = 96.46(2)°$, $\beta = 102.60(4)°$, $\gamma = 95.35(3)°$, $V = 1138(4)$ Å^3. However, the quality of the structure is poor, and so, no further discussion is warranted at this point.

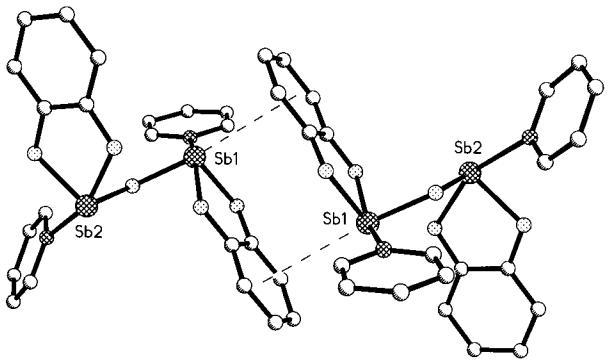

Figure 12. Extended structure of $[pySb(1,2\text{-}O_2C_6H_4)]_2O$, emphasizing the Sb···arene interaction.

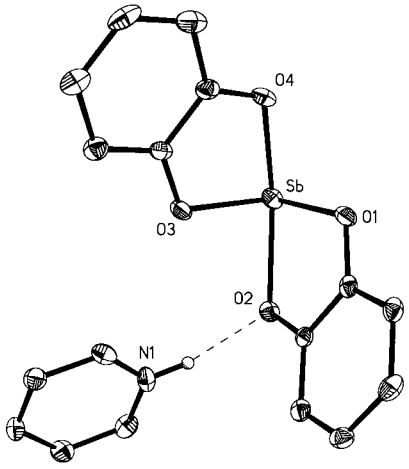

Figure 13. Molecular structure of $[pyH][Sb(1,2\text{-}O_2C_6H_4)_2]$.

Table 4. Selected Bond Lengths (Å) and Angles (deg) for $[Hpy][Sb(1,2\text{-}O_2C_6H_4)_2]$

Sb−O1	2.010(3)	Sb−O2	2.189(3)
Sb−O3	2.015(3)	Sb−O4	2.080(4)
O1−Sb−O2	77.9(1)	O2−Sb−O3	79.5(1)
O1−Sb−O3	99.3(1)	O2−Sb−O4	149.6(1)
O1−Sb−O4	84.1(1)	O3−Sb−O4	79.6(1)

The arene ring interacts symmetrically with the antimony, with an average Sb···C distance of 3.7 Å and an Sb··· centroid distance of 3.4 Å. Complexes with symmetric arene−Sb interactions are not common,[16] but examples are known for trihalide derivatives, for example, $(C_6Et_6)SbCl_3$ (Sb···centroid = 2.96 Å)[16a] and (9,10-dihydroantharcene)-$SbBr_3$ (Sb···centroid = 3.27 Å).[16b]

In the absence of water, $Sb(OAc)_3$ reacts with catechol in pyridine to give $[pyH][Sb(1,2\text{-}O_2C_6H_4)_2]$.[17] The molecular structure of $[pyH][Sb(1,2\text{-}O_2C_6H_4)_2]$ has been determined by X-ray diffraction, as illustrated in Figure 13. The antimony coordination environment in the anion $[Sb(1,2\text{-}O_2C_6H_4)_2]^-$ may be described as distorted trigonal bipyramid with a stereochemically active lone pair occupying an equatorial

(16) (a) Schmidbaur, H.; Nowak, R.; Huber, B.; Müller, G. *Organometallics* **1987**, *6*, 2266−2267. (b) Schmidbaur, H.; Nowak, R.; Steigelmann, O.; Müller, G. *Chem. Ber.* **1990**, *123*, 19−22. (c) Buslaev, Y. A.; Davidovich, R. L. *Koord. Khim.* **1989**, *15*, 1444−1465. (d) Schmidbaur, H.; Nowak, R.; Steigelmann, O.; Müller, G. *Chem. Ber.* **1990**, *123*, 1221−1226. (e) Probst, T.; Steigelmann, O.; Riede, J.; Schmidbaur, H. *Chem. Ber.* **1991**, *124*, 1089−1093.

Table 5. Crystal, Intensity Collection, and Refinement Data

	$[Sb_2(OCH_2CH_2O)_3]_n$	$[Sb(OCH_2CH_2O)(OAc)]_n$	$[pySb(1,2\text{-}O_2C_6H_4)]_2O$	$[pyH][Sb(1,2\text{-}O_2C_6H_4)_2]$
lattice	monoclinic	orthorhombic	triclinic	triclinic
formula	$C_6H_{12}O_6Sb_2$	$C_4H_7O_4Sb$	$C_{22}H_{18}N_2O_5Sb_2$	$C_{17}H_{14}NO_4Sb$
fw	423.66	240.85	633.88	418.04
space group	$P2_1/c$	*Pnma*	$P\bar{1}$	$P\bar{1}$
a/Å	6.562(1)	7.879(6)	9.615(1)	8.589(1)
b/Å	13.506(1)	7.267(5)	9.977(1)	9.534(1)
c/Å	12.511(1)	11.205(8)	13.947(2)	10.186(1)
α/°	90	90	104.481(2)	97.612(2)
β/°	100.982(2)	90	94.110(2)	99.689(2)
γ/°	90	90	117.127(2)	103.977(2)
V/Å^3	1088.4(2)	641.6(8)	1125.8(2)	784.6(2)
Z	4	4	2	2
temp (K)	243	243	243	238
radiation (*λ*, Å)	0.71073	0.71073	0.71073	0.71073
ρ(calcd), g cm^{-3}	2.585	2.494	1.870	1.769
μ(Mo Kα), mm^{-1}	4.966	4.240	2.435	1.778
θ max, deg	27.99	28.20	28.29	28.26
no. data	2425	721	4846	3502
no. params	128	51	281	209
R1	0.0219	0.0331	0.0356	0.0451
wR2	0.0518	0.0868	0.0552	0.0814
GOF	1.055	1.067	1.067	1.013

site. The Sb−O bond lengths are in the range 2.01−2.19 Å (Table 4), with the longest corresponding to the oxygen atom that is engaged in a hydrogen bonding interaction with the pyridinium counteranion, with an O···N distance of 2.73 Å. A similar antimony coordination geometry is observed for the related complex, $[NH_4][Sb(1,2\text{-}O_2C_6H_4)_2]$,[17a] and other derivatives.[18] It is noteworthy that the structure of $[Sb(1,2\text{-}O_2C_6H_4)_2]^-$ is similar to that of the arsenic analogue[19] but differs from the bismuth counterpart which exists as a dimeric species;[20] for $(pyH)[Sb(1,2\text{-}O_2C_6H_4)_2]$, the Sb···O distance between adjacent molecules is 3.53 Å so that it does not represent a significant interaction.

Experimental Section

General Considerations. All manipulations were performed using combinations of glovebox, high-vacuum, and Schlenk techniques.[21] Solvents were purified and degassed by standard procedures. $Sb(OAc)_3$ and $[Sb_2(OCH_2CH_2O)_3]_n$ were a gift from ATOFINA Chemicals, Inc. Ethylene glycol (Aldrich, 99.8%) and pyridine were dried over activated 4 Å molecular sieves. Catechol (Aldrich, 99%+) was dried by triturating several times with dry tetrahydrofuran, followed by drying in vacuo overnight. ^{1}H NMR spectra were recorded on a Bruker Avance 400 DRX spectrometer. ^{1}H chemical shifts are reported in ppm relative to $SiMe_4$ ($\delta = 0$) and were referenced internally with respect to the protio solvent impurity.

Crystallization of $[Sb_2(OCH_2CH_2O)_3]_n$. Crystals of $[Sb_2(OCH_2CH_2O)_3]_n$ suitable for X-ray diffraction were obtained by slow cooling of a solution in warm ethylene glycol.

Synthesis and Crystallization of $[Sb(OCH_2CH_2O)(OAc)]_n$. $[Sb(OCH_2CH_2O)(OAc)]_n$ was prepared by a literature method.[12] A solution of $Sb(OAc)_3$ (1.00 g, 3.35 mmol) in benzene (ca. 40 mL) was treated with a solution of ethylene glycol (0.21 g, 3.35 mmol) dissolved in benzene (ca. 20 mL), resulting in the rapid formation of a white precipitate. The mixture was stirred at room temperature overnight. The product was isolated and washed with benzene (ca. 20 mL) to give $[Sb(OCH_2CH_2O)(OAc)]_n$ (0.44 g, 55%). Crystals suitable for X-ray diffraction were obtained by sequentially layering a solution of $Sb(OAc)_3$ (1.00 g, 3.35 mmol) in THF (ca. 40 mL), a layer of THF (ca. 20 mL), and a layer of ethylene glycol (0.21 g, 3.35 mmol) in THF (ca. 30 mL). The mixture was left to stand, undisturbed, overnight, producing crystals of $[Sb(OCH_2CH_2O)(OAc)]_n$.

Synthesis and Crystallization of $[Hpy][Sb(1,2\text{-}O_2C_6H_4)_2]$. A mixture of catechol (0.74 g, 6.7 mmol) and $Sb(OAc)_3$ (1.00 g, 3.35 mmol) in pyridine (ca.. 25 mL) was stirred overnight. After this period, the volume of the yellow solution was reduced to ∼2 mL, at which point a large mass of yellow crystals formed. The mixture was filtered, and the yellow crystals of $[Hpy][Sb(1,2\text{-}O_2C_6H_4)_2]$ were washed with pentane (3 × 15 mL) and dried in vacuo (1.29 g, 92%).

Synthesis and Crystallization of $[Sb(1,2\text{-}O_2C_6H_4)]_2O$. A mixture of catechol (0.74 g, 6.7 mmol) and $Sb(OAc)_3$ (2.00 g, 6.7 mmol) was treated with pyridine (ca. 50 mL) in a Schlenk tube. Water (60 μL, 3.34 mmol) was added to the surface of the pyridine and allowed to diffuse into the solution for several minutes before stirring was initiated. The mixture was stirred for 4 days, over which period the initially pale yellow color of the solution fades and a floculant white precipitate forms. The solid was isolated by filtration, washed with benzene (ca. 30 mL), and dried in vacuo, giving $[pySb(1,2\text{-}O_2C_6H_4)]_2O$ (0.95 g, 45%) as a white solid. Crystals suitable for X-ray diffraction were obtained by allowing the combined filtrate and benzene washing to stand at room temperature. $[pySb(1,2\text{-}O_2C_6H_4)]_2O$ is insoluble in common solvents, but its composition is confirmed by ^{1}H NMR spectroscopic

(17) $[pyH][Sb(1,2\text{-}O_2C_6H_4)_2]$ has been previously reported but not structurally characterized. See: (a) Sen Gupta, A. K.; Bohra, R.; Mehrotra, R. C.; Das, K. *Main Group Met. Chem.* **1990**, *13*, 321−339. (b) Barnard, P. W. C.; Alamgir, M. *Nucl. Sci. Appl., Ser. B* **1981**, *12*−*13*, 41−46.

(18) (a) Yunjin, L.; Zhonghe, Z.; Da, G. *Yingyong Huaxue* **1987**, *4*, 61−64. (b) Yunjin, L.; Da, G. *Yingyong Huaxue* **1989**, *6*, 62−64.

(19) Shapski, A. C. *Chem. Commun.* **1966**, 10−12.

(20) Smith, G.; Reddy, A. N.; Byriel, K. A.; Kennard, C. H. L. *Aust. J. Chem.* **1994**, *47*, 1413−1418.

(21) (a) McNally, J. P.; Leong, V. S.; Cooper, N. J. In *Experimental Organometallic Chemistry*; Wayda, A. L., Darensbourg, M. Y., Eds.; American Chemical Society: Washington, DC, 1987; Chapter 2, pp 6−23. (b) Burger, B. J.; Bercaw, J. E. In *Experimental Organometallic Chemistry*; Wayda, A. L., Darensbourg, M. Y., Eds.; American Chemical Society: Washington, DC, 1987; Chapter 4, pp 79−98. (c) Shriver, D. F.; Drezdzon, M. A. *The Manipulation of Air-Sensitive Compounds*, 2nd ed.; Wiley-Interscience: New York, 1986.

(22) Sheldrick, G. M. *SHELXTL, An Integrated System for Solving, Refining and Displaying Crystal Structures from Diffraction Data*; University of Göttingen: Göttingen, Federal Republic of Germany, 1981.

analysis of a sample degraded in methanol-d_4 by addition of DCl in D_2O (2 drops of 20%) which revealed a 1:1 ratio of pyridine to catechol. Anal. Calcd for $C_{22}H_{18}N_2O_5Sb_2$: C, 41.7%; H, 2.9%; N, 4.4%. Found: C, 40.6%; H, 2.7%; N, 4.3%. IR Data (Nujol, cm^{-1}): 1600(w), 1592(w), 1577(w), 1249(vs), 1218(w), 1200(w), 1097(w), 1070(w), 1064(w), 1032(w), 1024(w), 1010(w), 1004(w), 908(w), 862(w), 790(m), 738(vs), 699(m), 694(m), 632(m), 619(w), 604(w), 545(w), 519(w), 467(w), 450(w), 417(w).

X-ray Structure Determinations. X-ray diffraction data were collected on a Bruker P4 diffractometer equipped with a SMART CCD detector. Crystal data, data collection, and refinement parameters are summarized in Table 5. The structures were solved using direct methods and standard difference map techniques and were refined by full-matrix least-squares procedures on F^2 with SHELXTL (Version 5.03).[22]

Summary

The molecular structures of antimony catalysts for the synthesis of PET by polycondensation of bis(hydroxyethyl)-terephthalate have been determined by X-ray diffraction. Specifically, the structures of both $[Sb_2(OCH_2CH_2O)_3]_n$ and $[Sb(OCH_2CH_2O)(OAc)]_n$ were determined to be polymeric, with the former complex forming two-dimensional sheets and the latter forming one-dimensional chains involving secondary Sb···O interactions. The dinuclear catecholate complex, $[pySb(1,2\text{-}O_2C_6H_4)]_2O$, obtained by reaction of $Sb(OAc)_3$ with catechol and water in pyridine, also possesses an extended structure. However, the structure differs from those of $[Sb_2(OCH_2CH_2O)_3]_n$ and $[Sb(OCH_2CH_2O)(OAc)]_n$ by also involving Sb···arene interactions with the benzene ring of a catecholate ligand.

Acknowledgment. We thank the National Science Foundation (Grant CHE 99-87432) for support of this research and Dr. Conor Dowling (ATOFINA Chemicals, Inc) for valuable and helpful comments.

Supporting Information Available: Crystallographic data. This material is available free of charge via the Internet at http://pubs.acs.org.

IC020204B